Proceedings of ISFOG 2025
5TH INTERNATIONAL SYMPOSIUM ON
FRONTIERS IN OFFSHORE GEOTECHNICS
Nantes, France | June 9-13 2025

ISBN 978-2-85782-758-0

Bearing capacity of the Yme GBS tank incorporating cyclic pore pressure accumulation with partial drainage

K.D.V. Huynh*
Norwegian Geotechnical Institute, Oslo, Norway

H.P. Jostad, H.J. Pederstad
Norwegian Geotechnical Institute, Oslo, Norway

P. Vabø, R. Daly, J.B. Gonzalez
Repsol Norge AS, Stavanger, Norway

V. Meyer
Formerly Norwegian Geotechnical Institute, Oslo, Norway
Statkraft AS, Oslo, Norway

**Khoa.D.V.Huynh@ngi.no (corresponding author)*

ABSTRACT: The Mobile Offshore Production Unit with Storage (MOPUstor) was installed at Yme Gamma in 2011, located 110 km from the Norwegian coastline in the Egersund basin in a water depth of 93 m. It was de-manned in 2012, and the MOPU (topside) was removed in 2016. For the Yme New Development project, it was necessary to evaluate the stability of the gravity base structure (GBS) storage tank without the MOPU. The GBS foundation includes external and internal skirts and a drainage system designed to relieve excess pore water pressures during cyclic loading. Front-End Engineering Design (FEED) for the new development indicated the need for significant ballast to ensure stability under storm conditions. This paper reassesses foundation stability using advanced finite element (FE) analyses. A 3D FE model of the GBS tank was developed using Abaqus. The Partially Drained Cyclic Accumulation Model (PDCAM) incorporated in Abaqus allowed a refined assessment of excess pore water pressures under design cyclic loading conditions. The FE analyses confirmed that the GBS tank meets stability requirements without additional ballast. Limiting equilibrium bearing capacity calculations were also performed to conservatively provide some preliminary estimates and to support the FE results. This study concludes that FE analysis combined with PDCAM can provide an effective and practical tool for evaluating foundation bearing capacity under cyclic loading in partially drained conditions.

Keywords: Gravity base structure, Cyclic bearing capacity; Pore pressure accumulation; PDCAM; Partial drainage

1 INTRODUCTION

The Yme field, located on the Norwegian Continental Shelf, is approximately 110 km from the Norwegian coastline in the Egersund basin in 93 m water depth. The MOPUstor (Mobile offshore Production Unit with Storage) was installed at Yme Gamma in 2011, de-manned in 2012 and the MPOU (topside) was removed in 2016. This change alters the loading condition on the foundation, necessitating a re-evaluation of the gravity base structure (GBS) storage tank's stability. Based on the original design back in 2008 and FEED in 2017, a horizontal sliding mechanism is expected to govern the stability of the Yme GBS tank, with direct simple shear (DSS) deformation mode at or below skirt tip level.

Although it is essential to account for cyclic loading effects on bearing capacity due to the generation of excess pore pressures, a widely accepted and practical calculation method is not currently available. While advanced numerical methods (Niemunis et al., 2005; Jostad et al., 2020; Saathoff and Achmus, 2024) can provide estimates, they are often too complex for practical engineering applications.

In the high-cycle accumulation model for sand (Niemunis et al., 2005), pore pressure accumulation is determined based on the tendency of accumulated plastic volumetric strain during drained cyclic loading. Under a partially drained analysis, this results in changes in pore pressure and effective stresses. The reduced effective stresses are then incorporated into the hypo-plasticity model (Niemunis and Herle, 1997) to calculate the resulting capacity or displacements.

An alternative approach is to use advanced constitutive models, such as SaniSand (Dafalias & Manzari, 2004), in a fully coupled consolidation

analysis. However, this requires analyzing each cycle within the time history, making it challenging to incorporate a safety factor into the analysis.

Therefore, a simplified and practical approach is needed to estimate accumulated excess pore pressures and the corresponding reduction in the undrained shear strength due to cyclic loads when calculating cyclic bearing capacity of offshore foundations.

This paper evaluates the cyclic bearing capacity of the Yme GBS tank using 3D FE analyses and limit equilibrium calculations, incorporating cyclic pore pressure accumulation with partial drainage during cyclic loading. The aim is to determine the minimum required submerged platform weight to resist the design environmental loading condition.

The foundation stability analyses used the same cyclic pore pressure accumulation technique with partial drainage, described in Andersen et al. (1994), as in the original foundation design and FEED. However, for this study, the technique was applied at each integration (material) point in the 3D finite element model of the foundation, rather than using an equivalent drainage length and a single cyclic shear strength for the considered soil layers.

2 SOIL DESIGN PARAMETERS

The soil stratigraphy at the Yme Gamma location is divided into four layers, as detailed in Table 1. For the bearing capacity analysis of the GBS tank under the ULS condition, the upper 10.0 m of the soil profile (sand and silt) is of primary importance.

The stability of the GBS tank depends on adequate cyclic soil strength, influenced by the drainage conditions for soil Unit I and especially Unit II. The main soil parameters for pore water pressure dissipation during cyclic loading are summarized in Table 1. The relative density and drained peak friction angles of these two soil units are given in Table 2. The friction angles differ for soils located beneath and outside of the foundation footprint, reflecting their dependency on consolidation stress.

Table 1. Static shear strength, permeability and modulus parameters for drainage during cyclic loading.

Unit	Depth (m)	s_u^{DSS} [1] (kPa)	k [2] (m/s)	M [3] (MPa)
I – Sand	0.0 – 2.5	-	$2 \cdot 10^{-4}$	80
II – Silt	2.5 – 10.0	110	$8 \cdot 10^{-6}$	50
III – Clay	10.0 – 16.0	110 – 200	-	-
IV – Clay	16.0 – 26.0	200 – 220	-	-

[1] Static undrained shear strength from DSS tests
[2] Coefficient of permeability
[3] Secant constrained modulus for reloading

Table 2. Relative density and drained peak friction angles of Unit I and II.

Unit	Relative density, D_r (%)	φ_p' (°) [1]	
		Beneath footprint	Outside footprint
I - Sand	70 – 80	38	42
II - Silt	80 – 10	34	38

[1] Drained peak friction angles

The cyclic contour data including the cyclic shear strain (γ_{cy}) and the accumulated permanent pore pressure (u_p) versus the number of cycles for both Unit I and Unit II were constructed from cyclic DSS tests with symmetric cyclic shear stress. The horizontal load components, critical for GBS sliding stability, have an average component close to zero, so there is no need for contour diagrams under non-symmetric cyclic shear stress. Moreover, since horizontal sliding failure is expected to control foundation stability, cyclic soil performance in triaxial compression or extension is less relevant. Therefore, the DSS tests from symmetric cyclic loading are sufficient for constructing the contour data used in the 3D FE-model of the Yme GBS for cyclic capacity analysis. Note that for other failure modes, different contour diagrams would be required.

3 PDCAM: BRIEF DESCRIPTION

The partially drained cyclic accumulation model (Jostad et al., 2015) has been implemented in the finite element program Abaqus as a user-defined material model. In the PDCAM FE calculation, the behaviour of an offshore foundation under idealized cyclic loading is analyzed using an explicit procedure that couples a cyclic undrained phase (applying only cyclic load components) with a time dependent consolidation phase (applying only average load components). Note that the average load components generally include the permanent loads (e.g., GBS weight, ballast weight), and the average component of the environmental loads.

Note that the cyclic phase is used to calculate the cyclic shear strength distribution based on the equivalent number of cycles, N_{eq}, and the average stress. N_{eq} represents the number of cycles of the current cyclic shear stress that gives the same accumulated pore pressure as when following the applied previous cyclic shear stress history (Andersen, 2015). The average stresses are calculated in the consolidation phase or assumed as an idealized stress distribution, ensuring equilibrium with the average loads. The average stresses consist of three main contributions: excess pore pressure, effective octahedral stress and average shear stress.

During the consolidation analysis using PDCAM, Abaqus calculates the pore pressure dissipation and

flow based on the excess pore pressure field and the consolidation parameters including permeability and constrained modulus. The main task of PDCAM is to determine the rate of the pore pressure generation due to cyclic loading for each material point. Here, "rate" refers to the time derivative of the pore pressure, i.e., the increase in pore pressure over a given time increment (number of cycles). However, instead of directly using this rate, PDCAM applies it as an equivalent volumetric strain rate. For undrained conditions, this is back-calculated as excess pore pressure; for fully drained conditions, it is presented as a volumetric strain. For partly drained conditions, a combination of pore pressures and volumetric strains is calculated by the finite element code. It is important to note that this is not a classical consolidation analysis, which is typically completed when the excess pore pressure is small. Instead, it is a time-dependent coupled pore water flow and stress equilibrium analysis (often referred to as consolidation analysis). The idealized time history is followed by time increments corresponding to a given number of cycles.

The general input data required for the PDCAM analysis include:

- Cyclic contour diagrams: pore pressure and cyclic shear strain contours versus the number of undrained cycles (N) and cyclic shear stresses normalized by effective octahedral consolidation stress ($\tau_{cy}/\sigma_{oct,c}$) (e.g., Anderson, 2015);
- Average (drained) volumetric and shear stress-strain relationships;
- Coefficient of consolidation;
- Idealized history of average and cyclic load components, i.e., parcels with a number of cycles at constant load amplitudes and average loads.

The PDCAM calculation procedure consists of an average consolidation phase followed by a cyclic phase for each loading parcel. This explicit coupling process is repeated iteratively until the final load parcel is reached.

4 PDCAM: VERIFICATION IN ABAQUS

PDCAM was previously implemented in the Plaxis finite element program. Its performance was demonstrated through back-calculations of cyclic laboratory tests and a centrifuge test of a gravity base structure on very dense sand (Jostad et al., 2015). This section presents the verification of PDCAM implementation in Abaqus, which was conducted at three levels: element test, one-dimensional (1D) test, and three-dimensional axisymmetric model. The element test verified the PDCAM's functionality at the material point. The 1D consolidation FE analysis confirmed that the cyclic shear stress levels followed the given loading parcels accurately, and that pore pressure accumulation and the equivalent number of cycles, N_{eq}, were calculated as expected. The three-dimensional axisymmetric FE-model representing the soil behaviours, drainage conditions, and pore pressure accumulation and dissipation around one of the single drains within the GBS foundation, was constructed. The aim of this analysis was to evaluate and verify the coupled pore fluid diffusion/stress analysis capability in the Abaqus program. Due to space constraints and also most relevant for this study, only the element test is presented in this section.

The pore pressure accumulation procedure was first tested in Abaqus for a material point. The Abaqus results were compared with both the Bifurc (NGI, 1999) and the expected outcomes directly extracted from the pore pressure contour diagrams.

The soil was assumed to be undrained. A constant normalized cyclic shear stress $\tau_{cy}/\sigma_{vc}' = 0.2$ was used to test the pore pressure accumulation, while $N_{eq} = 10$ was considered to verify the cyclic shear strain calculation.

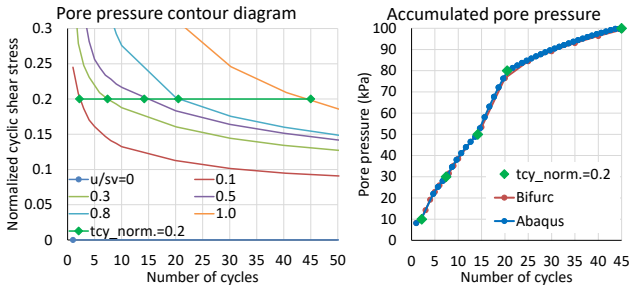

Figure 1. Comparison of input data of pore pressure versus number of cycles at τ_{cy}/σ'_{vc} = 0.2 (left) against calculated results using Bifurc and Abaqus (right).

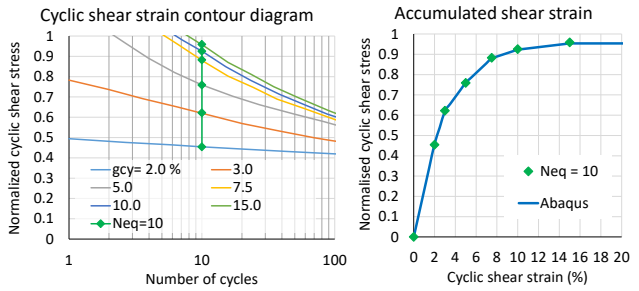

Figure 2. Comparison of input data of normalised cyclic shear stress versus cyclic shear strain at N_{eq} = 10 (left) against calculated results using Abaqus (right).

Figure 1 plots a comparison between the input data of pore pressure versus the number of cycles and the results calculated by using the Bifurc and Abaqus FE programs. These results are almost identical.

A very good agreement between the input data for the cyclic shear strain calculation and the Abaqus FE calculation for N_{eq} = 10 is also observed in Figure 2.

These results confirm PDCAM worked well for the element test, i.e., at the material point.

5 FE ANALYSIS OF GBS CAPACITY

5.1 FE model and calculation procedure

Figure 3 presents a full 3D FE-model of the Yme GBS tank constructed using Abaqus. The steel GBS has skirts penetrating 3.2 m into the seabed, leaving 0.3 m between the seabed and the platform base, which is filled with grout to even out contact stresses and remove water-filled voids. Filter panels in the skirt compartments facilitate drainage of excess pore pressures generated by cyclic loading.

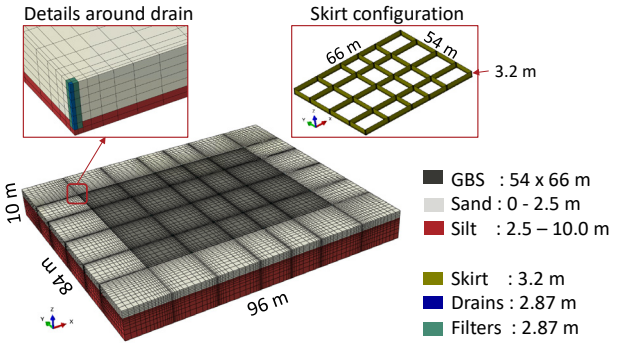

Figure 3. Overview of full 3D FE-model of Yme GBS tank.

The FE-model's bottom boundary was set 10.0 m below the seabed (bottom of the silt layer), with an outer boundary 15.0 m from the tank's periphery to minimize boundary effects. The bottom boundary was fully fixed, and the sides were constrained by roller boundaries. A zero pore pressure boundary condition was assigned at the top surfaces of the drains and the sand layer outside the GBS tank to allow free pore pressure dissipation.

In the PDCAM FE analyses, the skirts were fully constrained to the GBS base and modeled as a rigid body, assuming full roughness for interaction with the surrounding soils.

The design cyclic load cases covered storm build-up and decay in accordance with NORSOK N-003 requirements (NORSOK, 2007), represented as three- or four-hour time series. It is seen that the average loading is close to zero, meaning the tank is subjected to two-way cyclic loading. NGI performed load cycle counting on the provided time histories for design wave load case using the Rainflow method. The peak load was assumed to occur at the end of the storm, which is a conservative assumption from a bearing capacity perspective, as it maximizes the cyclic loading effect.

To evaluate the cyclic capacity of Yme GBS, the following coupled FE analyses were performed:

- Consolidation analysis: with zero average environmental load components, using PDCAM. The consolidation stress was calculated based on the GBS weight;
- Cyclic undrained capacity analysis: applying only cyclic load components with the Tresca material model. The safety factor, SF is set equal to the load scaling factor at failure under large displacements.

Due to computational limits, full iterative procedure between cyclic and consolidation analyses at each loading parcel was performed only at the end of the cyclic FE analysis and the end of the consolidation FE analysis. This conservative approach neglects the potential beneficial effect of cyclic shear stress redistribution at intermediate loading parcels. An iteration process ensures consistency between cyclic and consolidation analyses, as shown in Figure 4.

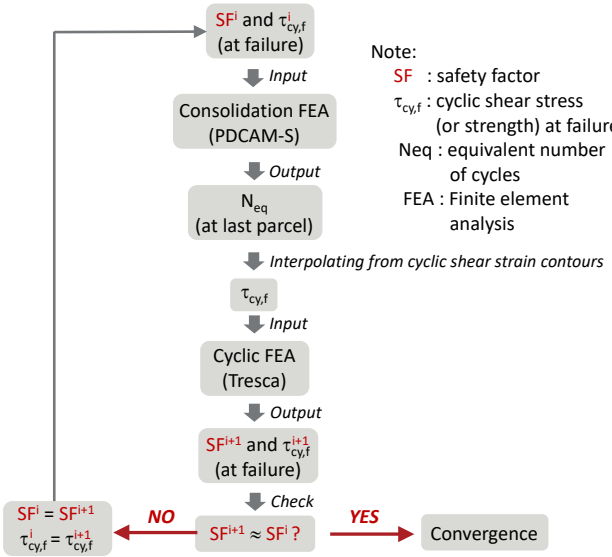

Figure 4. Iteration process for cyclic capacity analyses of GBS tank using Abaqus FE program.

5.2 FE results and discussion

5.2.1 Preliminary cyclic capacity FE analysis

As an initial assumption, the maximum cyclic shear stress of 52.4 kPa at the skirt tip (3.2 m below the seabed) obtained in the FEED phase (NGI, 2017) was applied to the consolidation FE analyses using the PDCAM material model. This cyclic shear stress corresponds to a sliding failure at the skirt tip, calculated assuming N_{eq} = 10 cycles in the entire silt layer (Unit II). A load spread of 1:3 was assumed to linearly distribute the cyclic shear stress and the GBS weight (23323 tonnes) in the silt beneath the skirted foundation. Figure 5 presents the distribution of the

calculated pore pressures and N_{eq} values in a vertical cross section at x = 0 m (middle of the FE-model) at the end of the consolidation analysis. The corresponding cyclic shear strengths interpolated from the cyclic shear strain contour diagrams are also shown in Figure 5. This figure indicates that accounting for the variation of N_{eq} could result in higher cyclic shear strengths, particularly around the periphery of the GBS tank, positively affecting the capacity analysis.

The cyclic shear strengths were then used in the cyclic FE analysis with the Tresca material model to compute the cyclic bearing capacity of the GBS tank. The load-displacement curve is plotted in Figure 6. The safety factor (i.e., a load scaling factor) was calculated to be 1.21. Figure 5 illustrates the shear stress, taken equal to the Tresca stress at failure calculated from the cyclic FE analysis, in the vertical cross section at x = 0 m. The cyclic shear stress distribution was then used as input for the next consolidation analysis.

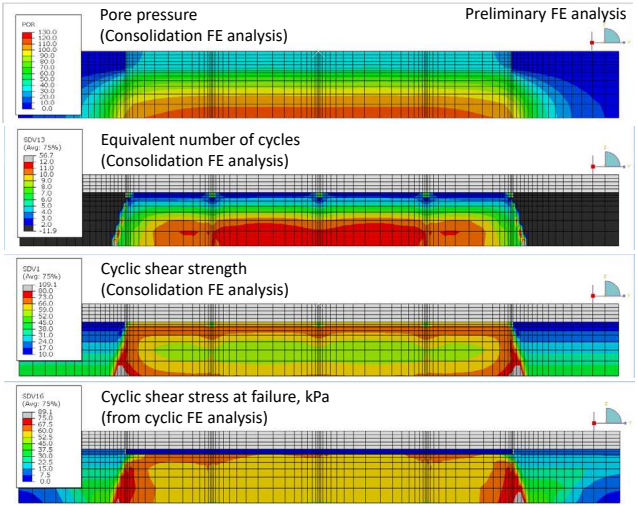

Figure 5. Distribution of pore pressure, N_{eq}, cyclic shear strength associated to N_{eq}, and cyclic shear stress in silt layer calculated from preliminary cyclic capacity FE analysis.

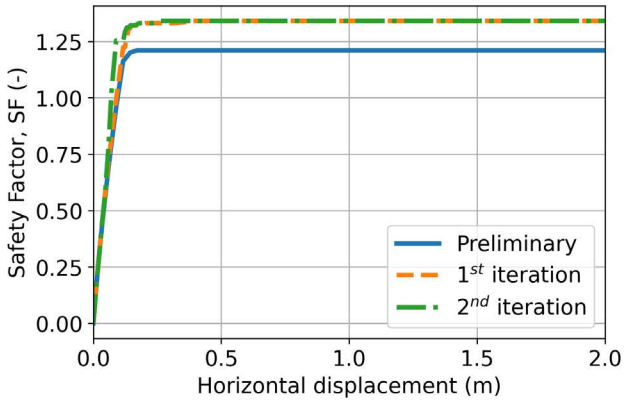

Figure 6. Load-displacement curve calculated from preliminary, 1st iteration and 2nd iteration of cyclic FE analysis with Tresca material model.

5.2.2 1st iteration of cyclic capacity FE analysis

Using the cyclic shear stress distribution from the preliminary cyclic FE analysis as inputs, the consolidation analysis with PDCAM was repeated. The calculated pore pressure distribution and N_{eq} values in the vertical cross section at x = 0 m are shown in Figure 7. The corresponding cyclic shear strengths, determined from the cyclic shear strain contour diagrams, are also plotted in Figure 7. The results indicate a slight increase in pore pressure and a reduction in N_{eq} values compared to the preliminary PDCAM FE analysis. These changes, along with the consideration of N_{eq} variation in the silt layer outside the 1:3 load spread, effectively enhanced the cyclic shear strength in the silt layer. These shear strengths were then used in the 1st iteration of cyclic analysis to determine the cyclic capacity of the GBS tank.

The load-displacement curve of the 1st iteration is plotted in Figure 6. With higher cyclic shear strength, the calculated safety factor increased from 1.21 to 1.34. Figure 7 illustrates the shear stress (Tresca stress) at failure in the vertical cross section at x = 0 m, calculated from the cyclic FE analysis. This cyclic shear stress was then used as input for the next iteration of the consolidation analysis.

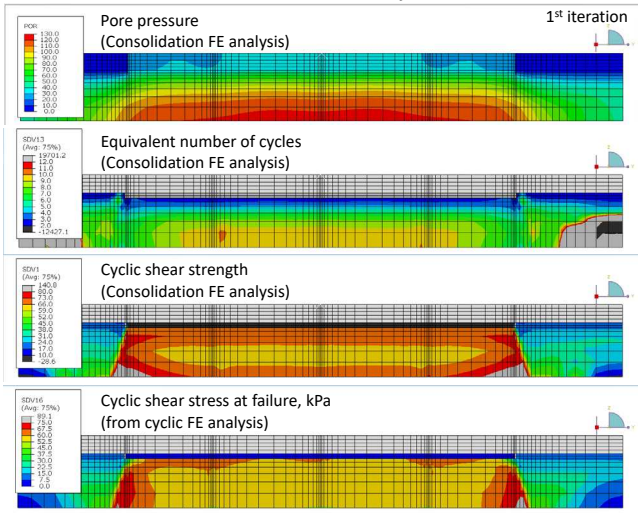

Figure 7. Distribution of pore pressure, N_{eq}, cyclic shear strength associated to N_{eq}, and cyclic shear stress in silt layer calculated from 1st iteration of cyclic capacity FE analysis.

5.2.3 2nd iteration of cyclic capacity FE analysis

Following the same calculation procedure as in the 1st iteration, the 2nd iteration of consolidation analysis using PDCAM indicated that the overall distributions of N_{eq} and cyclic shear strength were very similar to those in the 1st iteration.

Figure 6 plots the load-displacement curve calculated from the cyclic capacity FE analysis using the Tresca model. The calculated safety factor remained unchanged at 1.34, confirming the

convergence of the SF calculation. Figure 8 shows the deformed mesh and the calculated displacement at failure for this 2nd iteration. A view cut at x = 0 m, displaying the incremental shear strain at failure, indicates that a sliding failure occurred at 6.4 m below the seabed.

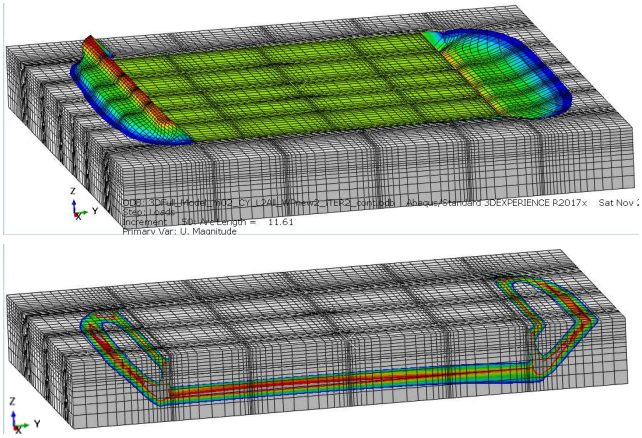

Figure 8. Deformed mesh and displacement (top) and incremental shear strain (bottom) at failure calculated from 2nd iteration (final) of cyclic capacity FE analysis.

6 LIMIT EQUILIBRIUM ANALYSIS

Limit equilibrium bearing capacity calculations were performed for sliding at varying depths below the footprint, accounting for the torsional moment, horizontal load, and differential seabed pressures. The geotechnical design was performed in accordance with NORSOK N-001 (NORSOK, 2012). Figure 9 shows the active and passive earth pressures and outer side shear used for distributing the torsional moment and horizontal load. Figure 10 shows the footprint area used in the calculations. The remaining torsional moment, after utilizing the active and passive earth pressures and the skirt wall friction, was assumed to be taken by the grey areas in Figure 10.

The calculations were carried out as follows:

- Active and passive earth pressures: used along the short sides of the foundation for distributing the torsional moment, down to skirt tip level. An earth pressure coefficient of 2.0 was used.
- Side shear: used along the front and back sides of the foundation down to the sliding level for distributing the torsional moment.
- Remaining torsional moment: distributed below the platform footprint.
- Shear strength below footprint: used to resist the horizontal load.
- Earth pressures for horizontal load: active and passive earth pressures along the GBS's front and back sides were used down to the sliding level.
- Side shear for horizontal load: used along the short sides of the foundation down to the sliding level.

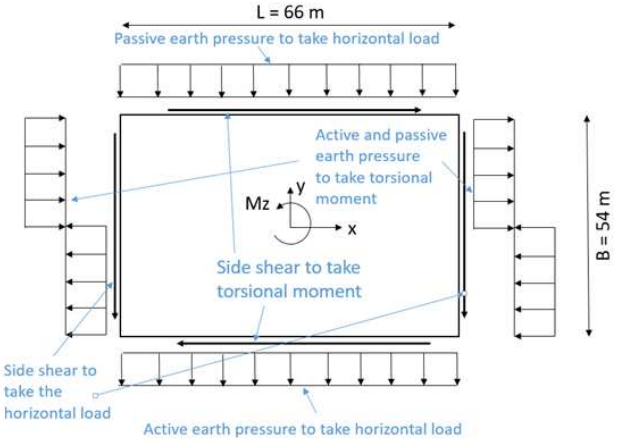

Figure 9. Distribution of active/passive earth pressures and side shear for distribution of torsional moment.

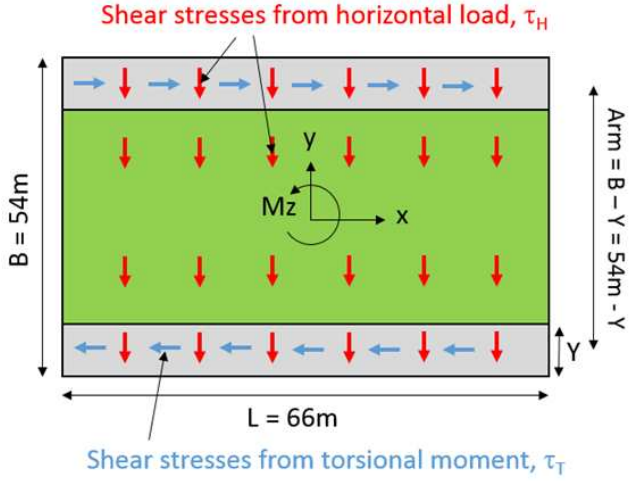

Figure 10. Footprint area used in stability calculations, assuming torsional moment taken by the shaded areas.

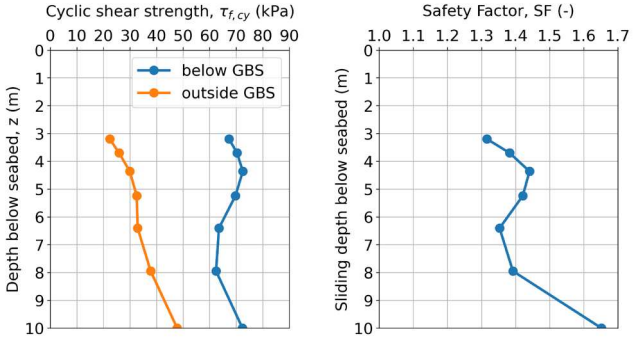

Figure 11. Cyclic DSS shear strength profiles of Unit II (left) and calculated factor of safety versus sliding depth below GBS foundation (right).

The cyclic strength of the soils was considered in the limiting equilibrium analyses as follows:

- Unit I (sand): below the platform footprint, the cyclic shear strength of Unit I is higher than Unit II at the skirt tip level, so it was disregarded in stability analyses. Outside the footprint, Unit I was modelled with equivalent

undrained shear strengths derived from drained parameters, expected to behave predominantly in a drained manner during design storm events.

Unit II (silt): The cyclic shear strength of Unit II plotted in Figure 11 is the key parameter, taken directly from the 3D FE analyses using PDCAM.

Horizontal sliding resistance was calculated at different depths to assess the governing sliding depth below the foundation. The calculations were performed for a platform on-bottom pressure of 64 kPa (zero ballast condition). Figure 11 indicates the lowest factor of safety is SF = 1.32 for sliding at skirt tip level (3.2 m) and SF = 1.35 for sliding at 6.4 m, aligning very well with the FE results in Section 5.2.3.

The results in this section indicate that limit equilibrium methods could be used in this case to determine sliding capacity. However, the main challenge lies in accurately estimating shear strength under partially drained cyclic loading.

7 CONCLUDING REMARKS

This study reassessed the stability of the Yme GBS tank under revised loading conditions following the removal of the MOPU. Key findings include:

- The Yme GBS tank, with an on-bottom weight of at least 23323 tonnes, satisfies stability requirements without needing additional ballast. This finding is highly beneficial for the project and demonstrates the advantages of using the FE method for a more refined analysis instead of the limit equilibrium method.
- Comparisons between FE results and simplified limit equilibrium calculations affirm the robustness and reliability of the FE approach.
- Accounting for cyclic pore pressure accumulation with partial drainage is crucial for accurately predicting the cyclic bearing capacity of offshore foundations in sand and silts.

The combination of advanced FE analysis and PDCAM offers an efficient and practical tool for assessing excess pore pressure accumulation and the cyclic bearing capacity of offshore foundations subjected to cyclic loading.

AUTHOR CONTRIBUTION STATEMENT

K.D.V. Huynh: Conceptualization, Methodology, Data curation, Formal Analysis, Investigation, Software, Visualization, Writing – Original draft. **H.P. Jostad**: Conceptualization, Methodology, Supervision, Validation, Reviewing and Editing. **H.J. Pederstad**: Conceptualization, Methodology, Data curation, Formal Analysis, Reviewing and Editing. **P. Vabø**: Reviewing and Editing. **R. Daly**: Reviewing and Editing. **J.B. Gonzalez**: Reviewing and Editing. **V. Meyer**: Project administration, Conceptualization, Methodology, Reviewing and Editing.

REFERENCES

Andersen, K.H. (2015). Cyclic soil parameters for offshore foundation design. The 3rd ISSMGE McClelland lecture. In *Frontiers in offshore geotechnics III*, ISFOG'2015, Meyer. Taylor & Francis Group, London, 978-1-138-02848-7, pp.5-82.

Andersen, K.H., Allard, M.A. & Hermstad, J. (1994). Centrifuge model tests of a gravity platform on very dense sand; II: Interpretation. 7th Int. Conf. on Behaviour of Offshore Structures. BOSS'94. Cambridge, Mass. Proc. Vol. 1, 255–282.

Dafalias, Y.F. and Manzari, M.T. (2004). Simple plasticity sand model accounting for fabric change effects. *Journal of Engineering mechanics*, *130*(6), pp.622-634.

Jostad, H.P., Dahl, B.M., Page, A., Sivasithamparam, N. and Sturm, H. (2020). Evaluation of soil models for improved design of offshore wind turbine foundations in dense sand. *Géotechnique*, *70*(8), pp.682-699.

Jostad, H., Grimstad, G., Andersen, K. and Sivasithamparam, N. (2015). A FE procedure for calculation of cyclic behaviour of offshore foundations under partly drained conditions. *Frontiers in offshore geotechnics III*,*1*, pp.153-172.

NGI (1999). Bifurc-3D. A finite-element program for 3-dimensional geotechnical problems. NGI report no.: 514065-1, Oslo, Norway.

Niemunis, A. and Herle, I. (1997). Hypoplastic model for cohesionless soils with elastic strain range. *Mechanics of Cohesive-frictional Materials: An International Journal on Experiments, Modelling and Computation of Materials and Structures*, *2*(4), pp.279-299.

Niemunis, A., Wichtmann, T. and Triantafyllidis, T. (2005). A high-cycle accumulation model for sand. *Computers and geotechnics*, *32*(4), pp.245-263.

NORSOK (2007). NORSOK N-003: Actions and action effects, Ed. 2, Sep. 2007.

NORSOK (2012). NORSOK N-001: Integrity of offshore structures, Ed. 8, Sept. 2012

Saathoff, J.E. and Achmus, M. (2024). Estimation of capacity decrease due to accumulated excess pore pressures around cyclically loaded offshore foundations in sand. *Ocean Engineering*, *294*, p.116733.